Hindawi
Mobile Information Systems
Volume 2022, Article ID 3499624, 9 pages
https://doi.org/10.1155/2022/3499624

Research Article

Three-Dimensional Visualization Analysis of Distributed Virtual Reality Taking into Account Grid Scientific Computing Model

Xinxin Jin and Daohua Zhang

Department of Electronic and Information Engineering, Bozhou University, Bozhou, China 236800

Correspondence should be addressed to Daohua Zhang; 2006020049@bzuu.edu.cn

Received 26 January 2022; Revised 10 March 2022; Accepted 15 March 2022; Published 11 April 2022

Academic Editor: Hye-jin Kim

With the in-depth development of the application of virtual reality technology, people have higher and higher requirements for the complexity and realism of virtual scene, which far exceeds the real-time processing ability of computer graphics hardware. Back to this, there is an urgent need to solve the contradiction between the complexity of the scene and the real-time interaction. In this paper, the real-time visualization of real-time distributed virtual reality is studied in many aspects. Starting with the analysis of the characteristics of real-time visualization technology of distributed virtual reality, this paper studies the system structure of real-time distributed virtual reality, puts forward the idea of realizing real-time distributed virtual reality visualization, introduces grid scientific computing model, and constructs a three-dimensional vertical visualization platform of distributed virtual reality. The visual analysis of virtual reality is carried out for the corresponding slope and corresponding geological conditions; the comprehensive analysis of spatial distribution is carried out by using three-dimensional visualization, the relevant contents of real-time display, and the generation and real-time display of realistic graphics. In order to increase the realism of 3D image, visibility judgment, and blanking technology, the level of detail model and texture mapping is used. The simulation results show that the grid scientific computing model is effective and can support the three-dimensional visual analysis of distributed virtual reality.

1. Introduction

With the continuous development of social economy, engineering construction has become more and more common, but there are still certain limitations in engineering construction supervision, construction effect, and safety monitoring [1]. Especially for the safety monitoring of the project, it is necessary to monitor the stability of the soil as well as to analyze the surrounding environmental influence factors [2]. Different from the construction in the plain, the construction in the mountainous area is often affected by many factors such as geology and construction process [3, 4]. It should be noted that there are still certain bottlenecks and limitations in the current monitoring methods and monitoring technology [5, 6]. Although the analysis results can be obtained through the corresponding external equipment and monitoring system, the degree of visualization is not high, and more importantly, the specific status and specific physical changes of the overall project cannot be obtained in all directions, and the actual project changes can hardly be fed back. Meanwhile, it is difficult to realize safety monitoring and geological time-space analysis [7, 8]. Therefore, effective safety supervision is the main development trend of realizing three-dimensional, real-time data collection and automation of data processing [9, 10]. Experts within the industry have also begun relevant exploration and research, such as the use of monitoring instruments to realize three-dimensional visual analysis of objects and computational analysis, but there is still no operational solution for safety monitoring in complex environments [11, 12]. The continuous development of computer technology has promoted the continuous improvement of technology in various fields [13, 14]. The use of grids for scientific computing is a new form of computing, which uses computers scattered in different locations to form a combined logical computer, that is, "physical distribution, logical

concentration", and each distributed computer is used as one of the important nodes to calculate network nodes and provide this service to users [15–17]. Commonly used network calculations are grid calculations, which are used by users online with various services. Traditional slice visualization has specific properties of three-dimensional data and two-dimensional data, and the information expressed simultaneously is relatively small and one-sided. There is no fixed connection between such adjacent information, and the three-dimensional fluctuation of reflection cannot be realized [18–20]. Therefore, the conversion is from a two-dimensional plane to a three-dimensional back. Meanwhile, it can effectively get rid of the limitations of three-dimensional data and two-dimensional attributes. A complete three-dimensional model can be made through specific three-dimensional data, which can ensure that the three-dimensional data under a series of scattered two-dimensional images can achieve omni-directional and full-view viewing [21, 22].

Distributed virtual reality is one of the popular types of visual analysis, so its spatial recognition, scientific calculation, and recognition have become the focus of domestic scholars. However, the scientific definition of how to use distributed computing to realize virtual reality has become a huge challenge, which can explain how to use distributed computing to realize virtual reality. At present, other classification methods are relatively single, and it is not accurate to obtain the characteristics of distributed virtual reality. The grid scientific computing model is applied to the scientific computing process of distributed virtual reality space recognition. This method can apply the distributed virtual reality as the current prior knowledge to the scientific computing process of distributed virtual reality space recognition according to the spatial characteristics of distributed virtual reality. The information gain method is used to obtain the distributed truth of the content of distributed virtual reality, and the grid scientific computing model is used to constrain the spatial weight, integrate the space with high meaning similarity with the distributed meaning information, and construct the spatial recognition scientific computing model of distributed virtual reality, respectively. By constructing a random forest spectral model system, the parallelization of the model greatly improves the efficiency and timeliness.

In view of these shortcomings and requirements, based on the grid scientific computing model, taking a hydropower project as the entry point, the three-dimensional visualization analysis is performed in the geological environment through the safety monitoring and analysis of it. In view of its complexity of the calculation and simulation, the distributed methods are used to carry out virtual reality simulations, monitoring and analyzing hydropower project slope safety data fields all day long in the form of three-dimensional cloud diagrams, realizing analysis and evaluation of safety, and aiming to provide three-dimensional safety visualized monitoring and analysis methods and technologies for hydropower project construction.

2. Basic Knowledge and Related Technology

2.1. Overview of Visualization and Virtual Reality Technology. As far as scientific computing is concerned, its essence is to gain insight and mining potential laws and phenomena in data through computational means. It orientates at not only the data itself, but also the analysis and understanding of the specific information used, and pure statistics on the data itself has made it difficult to find the potential law and information [23, 24]. The development of computer technology has made it possible to speed up complex calculations. Meanwhile, simple data summary tables can be replaced by intuitive visual images, which can actually highlight the accurate grasp and understanding of information. The in-depth development of three-dimensional technology allows people to feedback the three-dimensional data scene of the three-dimensional image through the three-dimensional image [25, 26].

The rendering and display of 3D scene algorithms can be carried out in two ways. One is to render according to the specific surface shape. Its essence is to construct the geometric unit in the middle by relying on the corresponding data field, and on this basis, the specific surface drawing is realized according to the specific three-dimensional graphics, such as the is surface of the hillside; the second is to construct a planar two-dimensional image through a three-dimensional data field, that is, to first generate a three-dimensional overall stereo image is surface. This method has a good fidelity effect, and the images projected to two dimensions can also ensure the integrity of the attributes, but the amount of calculation is too large, and the calculation time is correspondingly longer [27, 28].

For virtual reality technology, it is a fixed scene generated by computer technology, where multiple devices or display and equipment are used to achieve immersive analysis of the user and to achieve harmonious interaction with virtual objects or targets in the surrounding environment. The virtual reality scene generated in this way can be a simulation of the real world or can be a virtual world of fantasy. It has two special features, that is, immersion and interactivity, respectively. The immersion style takes the user as the first perspective, as if it actually exists in a fixed scene, allowing them to experience personally; the interactivity is that the user and the surrounding environment can communicate and interact, rather than simply passive changes.

In the related technologies of virtual reality, the three-dimensional reality becomes an important means to achieve immersion and is also a necessary way to enable people to have a first perspective. For the human body, stereo vision is produced by the corresponding binocular parallax, especially for two images with parallax; the brain is used for effective processing, which can realize the mutual viewing of the same point on the screen. Although the perspective can be processed through perspective and other methods, it still produces a certain amount of parallax. In the long run, it causes too heavy burden for the eyes. For stereoscopic reality, its essence is to use the same scene to calculate the corresponding perspective view from the left and right perspectives to generate two parallax images. Finally, according to the corresponding mobile device, the left and right eyes can see the corresponding images, thereby achieving an immersive three-dimensional sense.

The specific principle is shown in Figure 1. Assuming to initialize a three-dimensional space, by setting the original

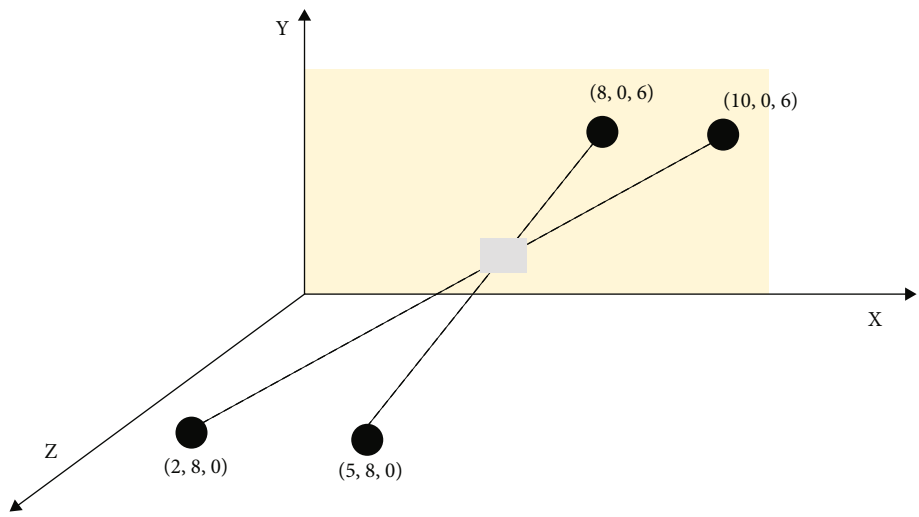

Figure 1: Schematic diagram of stereo display.

coordinates, left and right eyes, while analyzing the distance between the two eyes and projecting them into a specific XOY plane, it is clarified that the position of the object overlaps with the focus position of the left and right eyes. The specific image coordinates can be calculated by as

$$\begin{cases} x_{L_p} = (x_e - c/2) + (x - (x_e - c/2)) \times \dfrac{z_e}{z_e - z}, \\ x_{R_p} = (x_e - c/2) + (x - (x_e - c/2)) \times \dfrac{z_e}{z_e - z}, \\ y_{L_p} = y_{R_p} = y_e + (y - y_e) \times \dfrac{z_e}{z_e - z}. \end{cases} \quad (1)$$

Stereoscopic display is to further assist in the understanding and analysis of the attributes, spatial positions, and characteristics of the three-dimensional data. It is formed by the fusion of two specific left and right images; that is, by looking at the two images, more information about the perspective view can be obtained.

From the current development of scientific computing visualization, virtual reality provides basic support for the visualization of scientific and technical computing, which is an inevitable trend. Interactive visualization can be realized in the scene constructed by virtual reality technology, and corresponding information can be obtained more fully and more intuitively, and specific complex data can be further mined and analyzed.

In the virtual reality scene, the corresponding equipment can be used to observe the three-dimensional scene. It is to put yourself in the virtual reality three-dimensional scene, that is, to put yourself in the underground space, analyze the specific structure of the stratum, and realize the full interpretation and interpretation of the three-dimensional data, which is impossible to achieve by other display methods.

2.2. Grid Scientific Computing Model. The essence of the so-called network scientific computing is to use specific resources and site-related functions to implement high-level distributed grid computing to ensure the transmission and reception of data. The service layer of the network has nothing to do with specific resources and functions, but is related to specific regions and institutions. The specific network structure layer is used to realize the exchange of information services. Network application tools provide more specialized services and implementations. The specific application layer can be used by users to achieve specific development. Users can achieve customized development and use of network scientific computing through different levels of interfaces and service resources.

The specific relationship between each layer is shown in Figure 2:

In a specific campus network, users can perform a large number of calculations according to specific scientific experiment models, which requires high-performance grid scientific computing as support. Therefore, the grid scientific computing model can be used to effectively achieve rapid calculation and cost saving.

The grid scientific computing model uses a fixed network as the corresponding communication network and uses Ethernet and Fast Ethernet as the communication medium. Figures 3 and 4 show the basic functions of the specific server and grid node.

For the grid server, its specific task functions mainly include:

(1) Management tasks. When the server receives the corresponding tasks, the specific tasks can be divided into specific small units, and the assigned subtasks can be received and effectively processed. When all the subtasks are effectively processed, the final concrete result can be formed. During operation, the specific percentage and completion percentage can be displayed, and the completion of subtask nodes can be monitored simultaneously

(2) Manage nodes, including dynamic addition and withdrawal of nodes, and implement real-time detection and analysis of nodes

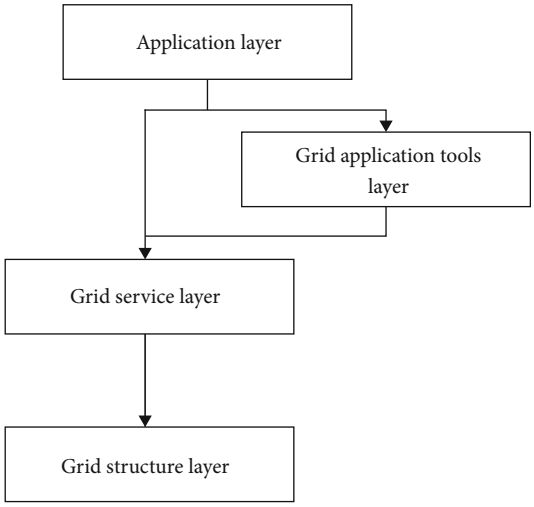

Figure 2: Hierarchical structure.

(3) Deal with various abnormal situations

(4) Realize grid computing in different scenarios through various API interfaces

(5) View the specific calculation status and final calculation result

For the grid node segment, its main functions are as follows:

(1) According to the corresponding calculation request, analyze the specific subtask and return the corresponding result

(2) Effectively process the divided subtasks

(3) Detect the specific responding server, and realize the fixed time data detection of the server through effective monitoring of the port, and feedback the corresponding result

For grid computing, the specific concurrent tasks that are executed do not need to be implemented at the specific command level, but are approached and analyzed through different subtasks. The specific steps are as follows, taking a fixed calculation parameter as an example for analysis:

2.3. Geological Conditions and Visual Analysis of Slope. Taking a hydropower project as an example, the surrounding environment is composed of corresponding metamorphic rocks and also includes specific crushed soil. Relatively speaking, the rock mass is relatively stable. However, after long-term weathering and solarization, the rock quality becomes soft and relatively loose. Meanwhile, according to the corresponding structural analysis, it can develop into more small faults.

In terms of specific natural structures, the relative weathering degree of the slope on the left is obviously affected by the surroundings, but the marble is relatively hard, indicating that it is affected by weathering and does not change much, while the green schist is and relatively soft due to its own texture, so it is greatly affected by the environment. Especially for the strongly weathered interlayer, it realizes specific development in specific distribution.

In terms of specific monitoring items, it mainly uses distributed virtual reality to monitor the following indicators, mainly including:

(1) Surface deformation monitoring points are used to realize deformation and slope deformation trends. The direction of the river is the specific X direction, the direction of the constant current is the Y direction, and the specific settlement deformation direction is the specific H direction

(2) A multipoint displacement meter is used to monitor the unloading relaxation deformation and local block sliding displacement of the shallow internal rock mass of the slope. The measuring point passes through the upper and lower walls of the main faults, which can effectively monitor the deformation of the blocks between the faults

(3) In the setting under specific observation conditions, the rock masses on the left and right banks are used for deformation observation; that is, visualization analysis is performed through distributed virtual reality three-dimensional dimension by arranging the corresponding observation piers when the left and right banks are fully visible

(4) In order to evaluate the corresponding effect, the monitoring effect of installation force measurement is analyzed by analyzing specific guidance, feedback, and corresponding prestress

3. Visualization Analysis of 3D Distributed Virtual Reality

Due to the randomness of the data collected and the splitting nature of the node characteristics, it is possible to ensure the construction of a visual analysis method with no connectivity between the determinants acquired, which can be used for scientific computing and have the features of initial parallelism. The scientific computing visual analysis algorithm for spatial recognition can effectively provide feedback on the decision parallelization, node parallelization, and feature selection. Parallelization processing is performed on the data collected based on the scientific computing visualization analysis method, which enables the parallelization of sample data in the computing process by dispersing a number of computer nodes. Compared with the traditional single machine recognition method, the method proposed in this paper can effectively save the I/O operation and avoid the excessive use of network bandwidth. In accordance with the data acquired from parallel computing, the idea of parallelization based on the scientific computing visualization analysis method is adopted in this paper to design a strategy for the parallel implementation of scientific computing

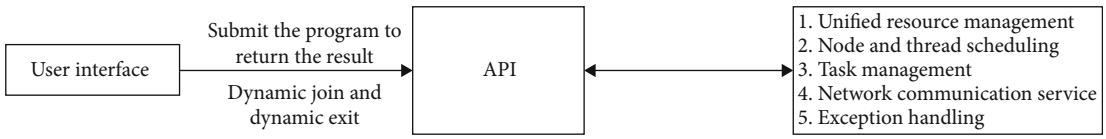

Figure 3: User grid diagram.

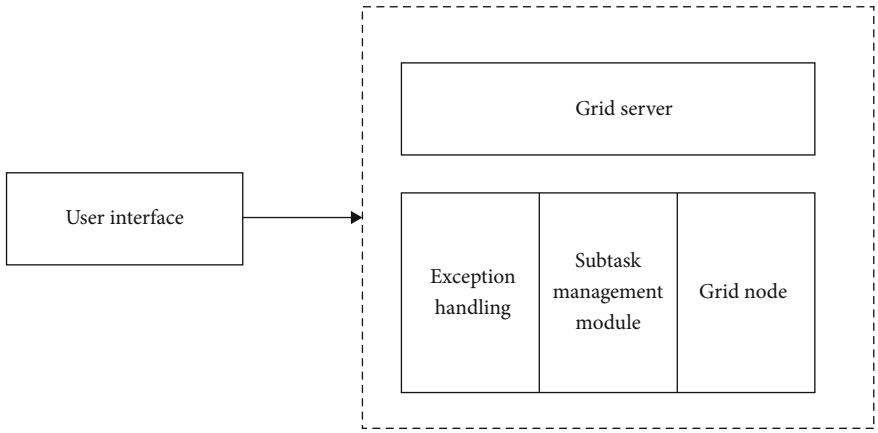

Figure 4: Server grid node diagram.

```
public void initialize( String[] args) {
   if( args.length ! =1) {
   System.err.println( "Args Error") ;
   System.exit( 1) ;
   }
   int digit=Integer.parseInt( args[0]) ;
   subjobNum=digit/9;
   for( int i=0; i<subjobNum; i++) {
   SubjobObject subj=new SubjobObject( i, i∗9) ; //Generation of subtask
   subjobList.add( subj) ;
   }
   }
Public boolean mergeSubjob( ) {//Merge subtask
   String finResult="3.";
   for( int i=0; i<subjobNum; i++) {
   SubjobObject subj=( SubjobObject) subjobList.get( i) ;
   finResult+=subj.subResult;
   }
   // output the final result
   outputResult(finResult);
   return true;
}
```

Algorithm 1:

visualization analysis by combining the framework features of the scientific grid computing model.

The parameters of the scientific grid computing model should be initialized and then perform the related operations based on the Baum-Welch algorithm. The results obtained by using the scientific computing visualization and analysis algorithm are highly dependent on the initial parameters. It is necessary to initialize the transformation matrix to determine whether 0 is obtained based on the transfer matrix or after the iterative operation. The sequence of observations is defined as $O = o_1 o_2, \cdots, o_T$, and the following can be obtained

$$P(O|\lambda) \geq P(O|\lambda) \tag{2}$$

where $P(O|\lambda)$ is calculated based on the forward-backward algorithm. With regard to the RFAM parameter λ and the state i, the forward probability $\alpha_t(i)$ is defined as the following:

$$\alpha_t(i) = P(o_1 o_2 \cdots o_T, q_t = i|\lambda) \tag{3}$$

where $\alpha_t(i)$ stands for the probability that the parameter A generates a sequence $(o_1 o_2,\cdots,o_t)$ and the state at time t is o_t.

Thus, $P(O|\lambda)$ can be calculated by using the following forward algorithm:

(1) Initialization

$$\alpha_1(j) = {}_j b_j(o_1), 1 \le j \le N. \tag{4}$$

(2) Recursion

$$\alpha_t(i) = b_i(o_t)\left[\sum_{j=1}^{N} \alpha_{t-1}(j)\alpha_{jt}\right], 2 \le t \le T, 1 \le i \le N. \tag{5}$$

(3) End

$$P(O|\lambda) = \sum_{j=1}^{N} \alpha T(j). \tag{6}$$

At the same time, $\beta_t(i)$ and $\xi_t(i,j)$ are defined as the following:

$$\beta_t(i) = P(o_{t+1} o_{t+2} \cdots o_T, |q_t = i, \lambda), \tag{7}$$

$$\xi t(i,j) = P(qt = i, qt + 1 = j|O, \lambda). \tag{8}$$

Based on the forward-backward algorithm, $\xi_t(i,j)$ can also be expressed as [2]

$$\xi t(i,j) = \frac{P(q_t = i, q_{t+1} = j|O,\lambda)}{P(O|\lambda)} = \frac{\alpha_t(i)\alpha_{ij} b_j(o_t + 1)\beta_{t+1}(j)}{P(O|\lambda)} = \frac{\alpha_t(i)\alpha_{ij} b_j(o_{t+1})\beta_{t+1}(j)}{\sum_{i=1}^{N}\sum_{j=1}^{N}\alpha_t(i)\alpha_{ij} b_j(o_{t+1})\beta_{t+1}(j)}. \tag{9}$$

The probability $\gamma_t(i,m)$ that the system is in the m-th mixed component of the state i at the moment t can be obtained as the following:

$$\gamma_t(i,m) = \left[\frac{\alpha_t(i)\beta_t(i)}{\sum_{i=1}^{N}\alpha_t(i)\beta_t(i)}\right]\left[\frac{\mu_{j,m} N\left(o_t, \mu_{j,m}, \Sigma j, m\right)}{\sum_{m=1}^{M}\omega_{j,m} N\left(o_t, \mu_{j,m}, \Sigma j, m\right)}\right]. \tag{10}$$

Firstly, the training set with the labels is used to train various types of RFAM, respectively. It is assumed that the types of scientific computation that requires spatial recognition is $k = \{1, 2,\cdots,K\}$, and then, the model parameter for each type is λ_k. The posterior probability is maximized based on the maximum likelihood criterion, while taking the Bayesian formula into consideration at the same time. Thus, the following can be obtained:

$$\bar{k} = \arg \max_{1\le k\le K} P(\lambda_k|O) = \arg \max_{1\le k\le K} \frac{P(O|\lambda_k)P(\lambda_k)}{P(O)}. \tag{11}$$

It is assumed that the prior probabilities $P(\lambda_k)$ of each type are the same. As $P(O)$ is irrelevant to k, the decision is omitted as the following.

$$\bar{k} = \arg \max_{1\le k\le K} P(O|\lambda_k). \tag{12}$$

As $P(O|\lambda_k)$ is very small, the overflow of the floating point can occur during the computer operation; its logarithmic value is often taken. With regard to multiple observation sequences, it is only necessary to perform weighting on the individual equations.

4. Results and Analysis

For the large tonnage and super long prestressed anchor cables excavated in hydropower projects, the main purpose is to control the deformation of the slope. Related dynamometers must be installed on the anchor cables at fixed intervals. According to relevant statistics, multiple anchor cable dynamometers are installed on the slope of the left bank.

The corresponding software is used to carry out effective statistics and generate monitoring results within a specific period. As some mobile devices may be damaged, data acquisition and analysis are only carried out for instruments that can work normally, and data analysis is carried out based on the data acquired by the instruments.

From the specific analysis results, after the anchor cable is fixed, the scope of its change can mainly include the following stages:

(1) The first is the rapid loss stage. For the loss of anchoring force, it is caused by the daily loss of anchoring force due to the loosening of the anchor cable steel strand or the daily loss of rock mass compression within the anchoring range

(2) For the fluctuation of the anchoring force, it mainly reflects that the amplitude of the anchoring force is small, which may cause contraction, rebound, and stress adjustment to achieve continuous repetition

(3) The steady change is mainly reflected in the anchoring force change tending to be stable and concretely showing a downward trend until it stabilizes. At this stage, part of the anchor cable will cause a large-scale change of anchoring force, which may be caused by the relative development of the rock mass in the environment and the interference of human factors caused by construction

Several sets (groups) of multipoint displacement gauges, anchor stress gauges, dislocation gauges, joint gauges,

reinforcement gauges, and strain gauges are arranged in the 3-layer shear-resistant tunnel to monitor the deformation of the shear-resistant tunnel, and osmotic pressure gauge is also arranged to monitor the groundwater level changes of the slope rock mass.

In view of the above analysis, a visual analysis of the results is carried out, with the aid of a specific elevation environment and corresponding equipment. The change of anchoring force of other cables is the corresponding negative values, which effectively represents that the anchoring force of this part is showing a downward trend. In terms of using the outlet in a specific environment to achieve a greater loss of anchoring force, a small increase appears in the anchoring force of other cables. In this case, the whole is in a relatively stable stage, and individual anchoring forces may change, which is caused by man-made construction interference. According to the corresponding calculation results, the results of the distributed virtual reality three-dimensional visualization analysis basically coincide with the actual detection results. From an overall point of view, due to the specific development of local rock masses in this part of the hydropower project area, the stress adjustment changes, and the specific anchor cable anchoring force is in the corresponding change and fluctuation stage, which coincide with the slope deformation monitoring results. Therefore, it can be seen from the results of the simulation experiment that the grid scientific computing model is effective.

4.1. Grid Scientific Computing. For three-dimensional visualization modeling, 15 computers are set up in a certain local area network as test equipment, of which 5 hosts and servers are in the same subnet, and 10 hosts are not in the same subnet. The connection is achieved through which appears the set gateway. The single processors are calculated and tested in series, respectively, and 40 decimal places are reserved for the specific calculation accuracy. The specific processing results are shown in Figure 5:

For a single processor, the specific calculation results are exactly the same as the distributed calculation results of the grid scientific computing model. In order to ensure the specific grid performance, the results of the specific processor operation are analyzed and compared with the calculations of the grid scientific computing model, and the network transmission time can be ignored. After comparison, the time taken by grid scientific calculation is significantly shorter than that of single processor calculation. The specific grid calculation time should meet the following:

$$T_{\text{The internet}} = \frac{T_{\text{stand-alone processing}}}{N}, \tag{13}$$

where, among them, N is the number of nodes in network computing.

From the specific experimental data, the grid scientific computing model is more efficient and effective.

4.2. Search of Mersenne Prime. For the three-dimensional model search, 15 machines are set as test equipment in a certain local area network. Among them, 5 hosts and servers are

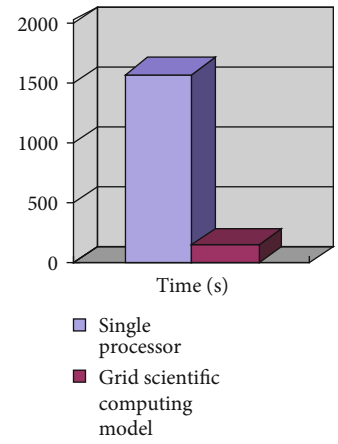

Figure 5: Calculated experimental results.

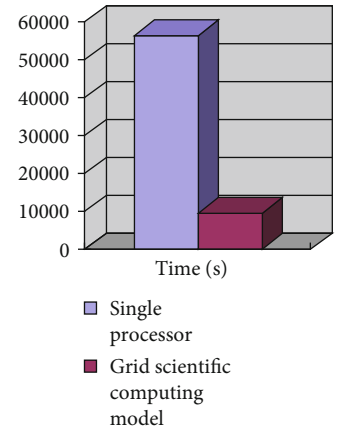

Figure 6: 3D model search experiment results.

in the same subnet, and 10 hosts are not in the same subnet. The connection with the server is realized through the set gateway. The analysis settings and initialization of the search are performed separately, and the calculation is performed from the specific grid scientific calculation model. Meanwhile, the single processor is used for serial calculation to search for the corresponding virtual reality three-dimensional model. The results obtained are shown in Figure 6:

5. Conclusion

In order to meet the growing needs in the fields of flight simulation, interactive GIS, virtual shopping, digital earth, and game entertainment, real-time distributed virtual reality visualization technology has become more and more important. Developed countries have always attached great importance to the development of virtual reality technology. Especially after the end of the Cold War, the transfer of investment focus has made the actual combat exercises subject to economic and political restrictions, prompted them to further study the new technology and environment of virtual reality, improve the experimental level of virtual reality, and made remarkable achievements. The virtual reality technology in China is still in its infancy. Although it has made

some achievements, there is still a big gap compared with developed countries. Therefore, it is urgent to develop the cause of virtual reality in China, and visualization technology is an important aspect of virtual reality.

Aiming at the problems existing in the visualization analysis of distributed virtual reality, this paper applies the grid scientific computing model to the visualization analysis of distributed virtual reality. Based on the detailed analysis of the characteristics of previous distributed virtual reality and combined with the characteristics of distribution, this method constructs the grid scientific computing model, mainly from the structure of the model. The data characteristics and the dynamic changes of the model are optimized to obtain the optimal parameters of the grid scientific computing model. Finally, the analysis of experimental results shows that the method proposed in this paper can carry out visual analysis according to the spatial state of distributed virtual reality. This method can effectively improve the timeliness and timeliness of scientific calculation of distributed virtual reality spatial recognition.

Data Availability

The data used to support the findings of this study are available from the corresponding author upon request.

Conflicts of Interest

The authors declare no conflicts of interest.

Acknowledgments

This study has been funded and supported by the 2020 Anhui Provincial Teaching Demonstration Course "Digital Image Processing Technology" (Project No: 1684); the Anhui Province Quality Engineering Information Technology Experimental Training Center (2019SXZX24); the Teaching Research Project (2019JYXM0275); the Key Program of Humanities and Social Science of Anhui Province (SK2019A0342); the 2021 Humanities and social Science Research Project of Anhui Universities (SK2021A0752); the Industry-university-research Cooperation Project of Bozhou University (BYC2021Z01); and the Bozhou University Key Natural Science Research Project (BYZ2019B01).

References

[1] S. West, M. Wagner, C. Engelke, and H. Horn, "Optical coherence tomography for the in situ three-dimensional visualization and quantification of feed spacer channel fouling in reverse osmosis membrane modules [J]," *Journal of Membrane Science*, vol. 498, no. 3, pp. 345–352, 2016.

[2] A. Bria, G. Iannello, L. Onofri, and H. Peng, "TeraFly: real-time three-dimensional visualization and annotation of terabytes of multidimensional volumetric images [J]," *Nature Methods*, vol. 13, no. 3, pp. 192–194, 2016.

[3] Y. Morisada, T. Imaizumi, and H. Fujii, "Determination of strain rate in friction stir welding by three-dimensional visualization of material flow using X-ray radiography[J]," *Scripta Materialia*, vol. 106, no. 5, pp. 57–60, 2015.

[4] I. Van Cruyningen, A. Lozano, M. G. Mungal, and R. K. Hanson, "Three-dimensional visualization of temporal flow sequences," *AIAA Journal*, vol. 29, no. 3, pp. 479–482, 1991.

[5] J. L. Byl, R. Sholler, J. M. Gosnell, B. P. Samuel, and J. J. Vettukattil, "Moving beyond two-dimensional screens to interactive three-dimensional visualization in congenital heart disease," *The International Journal of Cardiovascular Imaging*, vol. 36, no. 8, pp. 1567–1573, 2020.

[6] J. Strong and A. P. Dickin, "Three-dimensional visualization of top-down superimposed thrust sheets in the SW Grenville Province, Ontario," *Geological Magazine*, vol. 157, no. 2, pp. 149–159, 2020.

[7] Q. Cheng, L. Wei, Z. Liu et al., "Operando and three-dimensional visualization of anion depletion and lithium growth by stimulated Raman scattering microscopy," *Nature Communications*, vol. 9, no. 1, pp. 109–118, 2018.

[8] J. Y. Liu, J. L. Gong, L. Qin, B. Guo, and Y. Wang, "Three-dimensional visualization of subsurface defect using lock-in thermography," *International Journal of Thermophysics*, vol. 36, no. 5-6, pp. 1226–1235, 2015.

[9] C. K. Lee, S. Moon, S. Lee, D. Yoo, J. Y. Hong, and B. Lee, "Compact three-dimensional head-mounted display system with Savart plate," *Optics Express*, vol. 24, no. 17, pp. 19531–19544, 2016.

[10] K. Van Wieren, H. N. Tailor, V. F. Scalfani, and N. Merbouh, "Rapid access to multicolor three-dimensional printed chemistry and biochemistry models using visualization and three-dimensional printing software programs," *Journal of Chemical Education*, vol. 94, no. 7, pp. 964–969, 2017.

[11] C. Jiang, X. Liu, W. Wang, W. Wei, and M. Duan, "Three-dimensional visualization of the evolution of pores and fractures in reservoir rocks under triaxial stress," *Powder Technology*, vol. 378, no. 3, pp. 585–592, 2021.

[12] J. C. Lu, G. J. Ensing, R. G. Ohye et al., "Stereoscopic three-dimensional visualization for congenital heart surgery planning: surgeons' perspectives [J]," *Journal of the American Society of Echocardiography*, vol. 33, no. 6, pp. 775–777, 2020.

[13] H. Shimojo, T. Gonjo, J. Sakakibara, Y. Sengoku, R. Sanders, and H. Takagi, "A quasi three-dimensional visualization of unsteady wake flow in human undulatory swimming [J]," *Journal of Biomechanics*, vol. 93, no. 4, pp. 60–69, 2019.

[14] L. Z. Reinitz, B. Szőke, E. É. Várkonyi, P. Sótonyi, and V. Jancsik, "Three-dimensional visualization of the distribution of melanin-concentrating hormone producing neurons in the mouse hypothalamus [J]," *Journal of Chemical Neuroanatomy*, vol. 71, no. 3, pp. 20–25, 2016.

[15] X. Liu, Y. Wang, M. Tang, Y. Liu, L. Hu, and Y. Gu, "Three-dimensional visualization of coronary microvasculature in rats with myocardial infarction [J]," *Microvascular Research*, vol. 130, no. 3, p. 103990, 2020.

[16] K. Togami, T. Daisho, Y. Yumita, A. Kitayama, H. Tada, and S. Chono, "Evaluation of various tissue-clearing techniques for the three-dimensional visualization of liposome distribution in mouse lungs at the alveolar scale [J]," *International Journal of Pharmaceutics*, vol. 562, no. 2, pp. 218–227, 2019.

[17] J. W. Bai and C. Chi, "A social network image classification algorithm based on multimodal deep learning," *International Journal of Computers Communications & Control*, vol. 15, no. 6, pp. 1–12, 2020.

[18] Y. M. Lin, C. Song, and G. C. Rutledge, "Direct three-dimensional visualization of membrane fouling by confocal

laser scanning microscopy," *ACS Applied Materials & Interfaces*, vol. 11, no. 18, pp. 17001–17008, 2019.

[19] A. Acuna, M. A. Drakopoulos, Y. Leng, C. J. Goergen, and S. Calve, "Three-dimensional visualization of extacellular matrix networks during murine development [J]," *Developmental Biology*, vol. 4, no. 2, pp. 1–8, 2018.

[20] C. Ciurea, L. Pocatilu, and F. G. Filip, "Using modern information and communication technologies to support the access to cultural values," *Journal of System and Management Sciences*, vol. 10, no. 2, pp. 1–20, 2020.

[21] Y. Liu, "Three-dimensional visualization of carbon networks in nanocomposites," *Nanotechnology*, vol. 26, no. 44, p. 442501, 2015.

[22] J. A. Kaufman, M. J. Castro, N. Sandoval-Skeet, and L. Al-Nakkash, "Optical clearing of small intestine for three-dimensional visualization of cellular proliferation within crypts [J]," *Journal of Anatomy*, vol. 4, no. 8, pp. 1–9, 2017.

[23] P. H. Wang, T. H. Ying, P. C. Wang, I. C. Shih, L. Y. Lin, and G. D. Chen, "Obstetrical three-dimensional ultrasound in the visualization of the intracranial midline and corpus callosum of fetuses with cephalic position.[J]," *Prenatal Diagnosis*, vol. 20, no. 6, pp. 518–520, 2000.

[24] T. Bauch, P. Vijayaraman, G. Dandamudi, and K. Ellenbogen, "Three-dimensional printing for invivo visualization of his bundle pacing leads [J]," *American Journal of Cardiology*, vol. 116, no. 3, pp. 485-486, 2015.

[25] K. G. Cologne, J. Zehetner, L. Liwanag, C. Cash, A. J. Senagore, and J. C. Lipham, "Three-dimensional laparoscopy: does improved visualization decrease the learning curve among trainees in advanced procedures?," *Surgical Laparoscopy, Endoscopy & Percutaneous Techniques*, vol. 25, no. 4, pp. 321–323, 2015.

[26] C. Phatak, Y. Liu, E. B. Gulsoy, D. Schmidt, E. Franke-Schubert, and A. Petford-Long, "Visualization of the magnetic structure of sculpted three-dimensional cobalt Nanospirals," *Nano Letters*, vol. 14, no. 2, pp. 759–764, 2014.

[27] K. Obase, V. Jeevanandam, K. Saito et al., "Visualization and measurement of mitral valve chordae tendineae using three-dimensional transesophageal echocardiography from the transgastric approach [J]," *Journal of the American Society of Echocardiography*, vol. 28, no. 4, pp. 449–454, 2015.

[28] J. Dai, Y. An, and Z. Song, "Visualization 2: absolute three-dimensional shape measurement with a known object," *Optics Express*, vol. 25, no. 9, pp. 10384–10396, 2017.